

## SINGLE-ISOBAR PRODUCTION IN PROTON-PROTON INTERACTIONS AT 28.5 GeV/c\*

W. E. Ellis, D. J. Miller, T. W. Morris, R. S. Panvini, and A. M. Thorndike

Brookhaven National Laboratory, Upton, New York

(Received 29 July 1968)

Two- and four-prong final states in a 28.5-GeV/c  $p$ - $p$  bubble-chamber experiment were examined for single-isobar production in various decay channels; results are compared with missing-mass-spectrometer data. The 1400 enhancement was found to be an  $N\pi$  system with the ratio  $n\pi^+/p\pi^0 \sim 2$ , which establishes the isospin assignment  $I = \frac{1}{2}$ . The final state  $\Delta^{++}(1238)n$  was measured and compared with low-energy data to show that the cross section decreases according to  $P_{\text{lab}}^{-(1.91 \pm 0.08)}$ , consistent with single-pion exchange.

Several missing-mass-spectrometer experiments<sup>1,2</sup> have produced evidence for single-isobar production at energies ranging from 6 to 30 GeV. The most interesting structure seen is the strong,  $\geq 200$ -MeV wide enhancement near 1400 MeV, which is produced with a steep exponential dependence on  $t$ , the square of the four-momentum transfer.<sup>3</sup> This enhancement has not received solid endorsement as a resonance since its position at the low-mass end of the spectrum suggests that it can be interpreted as a kinematic effect.<sup>4</sup>

We report here an investigation of  $\sim 12\,000$  two- and  $\sim 12\,000$  four-prong events from a 28.5-GeV/c, 83 000-picture,  $pp$  exposure in the Brookhaven National Laboratory 80-in. hydrogen bubble chamber. We find that the enhancement at 1400 MeV is nearly all  $n\pi^+$  and  $p\pi^0$  in the ratio  $n\pi^+/p\pi^0 \sim 2$ , as expected for an isospin- $\frac{1}{2}$  system. An enhancement centered at  $\sim 1450$  MeV also occurs at the low-mass end of the  $p\pi^+\pi^-$  effective-mass spectrum. This peak is produced prominently at low  $t$  and has a cross section appreciably smaller than that of the 1400-MeV enhancement in the  $n\pi^+$  and  $p\pi^0$  systems. An additional enhancement is seen in the mass interval 1600-1700 MeV in both two- and four-prong events whose dependence on  $t$  is much less steep than that of the 1400- and 1450-MeV objects, in agreement with the counter data. The production of the  $\Delta^{++}$  resonance at 1238 MeV was observed in the final state  $\Delta^{++}(1238)n$ . Our cross section for this reaction combined with cross sections measured at lower energy is in agreement with the momentum dependence  $P_{\text{lab}}^{-2}$  expected for single-pion exchange. The 1520- and 2190-MeV isobars seen with the missing-mass spectrometers have too little cross section to be resolved in our data.

Calculations by Berger relating to the 1400 question in our data are presented in the following Letter.<sup>4</sup>

The reactions relevant to our study are

$$p + p \rightarrow p + (n + \pi^+), \quad (1)$$

$$\rightarrow p + (p + \pi^0), \quad (2)$$

$$\rightarrow p + (n + \pi^+ + \pi^0), \quad (3)$$

$$\rightarrow p + (p + \pi^0 + \pi^0), \quad (4)$$

$$\rightarrow (p + \pi^+) + n, \quad (5)$$

$$\rightarrow p + (p + \pi^+ + \pi^-). \quad (6)$$

The parentheses indicate the systems of particles whose mass spectra are to be studied. In all but (5), which is intrinsically isospin  $\frac{3}{2}$ , we expect the isospin- $\frac{1}{2}$  channels to dominate according to the usual observation that reactions that require quantum-number exchange decrease in cross section with increasing energy.<sup>5</sup>

The measuring accuracy at this energy is limited by the small curvature of high-momentum tracks.<sup>6</sup> Because of this and other limitations, the following items are noted:

(1) Reaction (6) is studied after making four-constraint kinematic fits to the data and selecting only those events with  $(p\pi^+\pi^-)$  in the backward hemisphere (targetlike). This selection avoids biases due to losses in data associated with short recoil-proton tracks from the half of the data where  $(p\pi^+\pi^-)$  is in the forward hemisphere (beamlike).

(2) Since kinematic fits to final states with one neutral particle are much less certain than fits to all charged-particle states, we rely on missing-mass techniques. Because of the beam-target symmetry we expect that half the events are of the type

$$p + p \rightarrow p_R + MMX, \quad (7)$$

where  $p_R$  is a low-momentum (recoil) proton and  $MMX$  is the low-mass system or isobar, with one or three charged tracks and possibly one or more neutrals. Figure 1(a) is a plot of  $MMX$  for

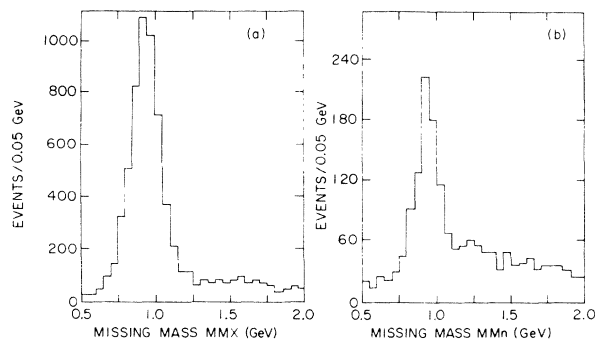


FIG. 1. (a) Missing mass  $MMX$  in the two-prong reaction  $p+p \rightarrow p(\text{recoil})+MMX$ . (b) Missing mass  $MMn$  in the reaction  $p+p \rightarrow p(\text{recoil})+\pi^++MMn$  from two-prong events.

two-prong events. The elastic final state dominates, giving a peak in  $MMX$  at  $\sim 940$  MeV and width of  $\sim \pm 100$  MeV; the width indicates the resolution in the measurement of  $MMX$  for higher masses as well. This resolution is comparable with that of the counter experiments at the same energy.<sup>1</sup>

To study  $MMX$  further in the two-prong events we look at all events that are kinematically compatible with the reaction

$$p+p \rightarrow p_R + \pi^+ + MMn, \quad (8)$$

where  $p_R$  is the slow recoil proton as before, the other track (of relatively high momentum) is assumed to be a  $\pi^+$  for this calculation, and  $MMn$  is the desired neutral missing mass. In Fig. 1(b) is shown a plot of  $MMn$  that reveals a distinct neutron peak with a resolution also about  $\pm 100$  MeV. This enables us to select the final state  $p n \pi^+$  by choosing the events with  $MMn$  within the neutron peak. Most of the events constituting the neutron peak also give reliable one-constraint kinematic fits to the final state  $p n \pi^+$ . The  $p p \pi^0$  final state cannot be studied directly, since no  $\pi^0$  peak is resolved in the neutral missing-mass distribution when the high-momentum track is interpreted as a proton.

We restrict our study to "forward isobar" events, since choosing the symmetric counterparts to Reactions (7) and (8), wherein  $p_R$  becomes a high-momentum proton, gives very poor resolution on  $MMX$  and  $MMn$ . Although the method just described is essential for studying the two-prong Reactions (1) through (5), a loss of events occurs with  $t \lesssim 0.06(\text{GeV}/c)^2$  due to a scanning bias against very short recoil-proton tracks.

(3) The structure in  $MMX$  for masses above the

elastic peak in two-prong final states can be seen more clearly if we remove the elastic events from the sample. Even though the resolution on  $MMX$  is  $\sim \pm 100$  MeV, the elastic final state is so dominant that some of the "tail" in the elastic distribution would obscure the low-mass region. The events that were removed were those which gave four-constraint kinematic fits to the elastic interpretation. A check, using coplanarity, showed no significant elastic contamination remaining for  $MMX > 1250$  MeV.

With the techniques and within the restrictions cited above, several results follow:

(a) We examine  $MMX$  of Reaction (7) and compare with the results of Anderson et al. at 30 GeV/c.<sup>1</sup> Figure 2(a) shows  $MMX$  from all two- and four-prong events for  $t > 0.06$  (GeV/c)<sup>2</sup> along with a solid curve that shows the counter results on the same scale as our data, integrated over the same  $t$  region. The cut on  $t$  is chosen to include a region in which scanning losses are slight [see item (2) above]. The shaded histogram in Fig. 2(a) shows the contribution of the four-prongs alone. This comparison shows that our two-prong data adequately account for the structure seen at low mass in the counter data. The four-prong data, as will be substantiated below, contribute little in the 1400 region, implying that the 1400 enhancement is made up of  $N\pi\pi$  or higher multiplicity.

(b) Since the low-mass region appears to be almost entirely an  $N\pi$  system, we explore the two-prong data in more detail.

The main histogram in Fig. 2(b) represents  $MMX$  in Reaction (7), while the shaded histogram represents the effective mass of  $\pi^+ + MMn$  in Reaction (8) using only the events where  $0.80 < MMn < 1.08$  GeV (neutron band). Both plots are restricted to events with  $t < 0.12$ . The same plots are shown for comparison in Fig. 2(c) for  $0.12 < t < 1.0$ . Note that  $MMX$  for two-prong events contains the systems indicated by parentheses in Reactions (1) through (4), while  $\pi^+ + MMn$  with the above restriction on  $MMn$  represents the effective mass of  $n\pi^+$ .

A broad enhancement centered at about 1400 MeV is apparent in the low- $t$  data. For  $t > 0.12$  an enhancement appears in the 1600- to 1700-MeV region. This behavior is in agreement with the counter results,<sup>1</sup> which indicate a very steep exponential slope for the production of the 1400 structure ( $\sim 2$  times the elastic slope) and a small slope for the 1690 structure ( $\sim \frac{1}{2}$  times the elastic slope). To determine the relative contributions

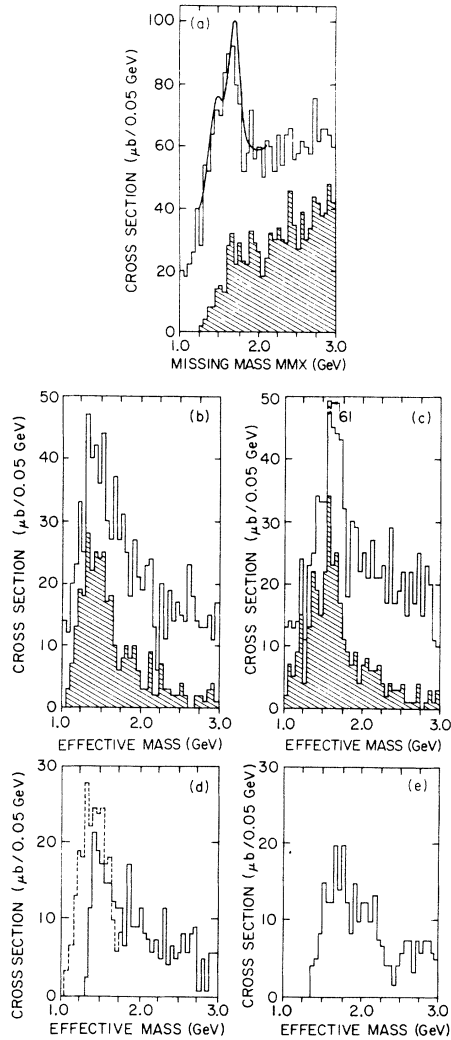


FIG. 2. (a) Missing mass  $MMX$  in four-prong events (shaded) and in two- plus four-prong events (main histogram) at values of  $t > 0.06$   $(\text{GeV}/c)^2$ . The smooth curve is the counter data of Anderson *et al.* integrated over the same  $t$  region (Ref. 1). (b) Effective mass of  $(MMn + \pi^+)$  (shaded) for  $MMn$  in neutron band  $(0.80 < MMn < 1.08)$  and  $MMX$  in two-prong events (main) with  $t < 0.12$   $(\text{GeV}/c)^2$ . (c) Same as (b) with  $t > 0.12$   $(\text{GeV}/c)^2$ . (d)  $p\pi^+\pi^-$  effective mass in the reaction  $p + p \rightarrow p + p + \pi^+ + \pi^-$  (solid line) and  $n\pi^+$  effective mass in  $p + p \rightarrow p + \pi^+ + n$  (dashed line), both for  $t < 0.12$   $(\text{GeV}/c)^2$ . (e) Same as (d) (solid line) for  $t > 0.12$   $(\text{GeV}/c)^2$ .

from Reactions (1) through (4) in the 1400-MeV region we count the number of events in the interval between 1250 and 1550 MeV where elastic background is no longer a problem [see item (3) above] from the low- $t$  histograms, Fig. 2(b), for  $MMX$  and  $(MMn + \pi^+)$ . The number of events in the peak in  $MMX$  is 235 and in  $(MMn + \pi^+) \equiv (n\pi^+)$  is 142. Assuming the  $MMX$  system is entirely

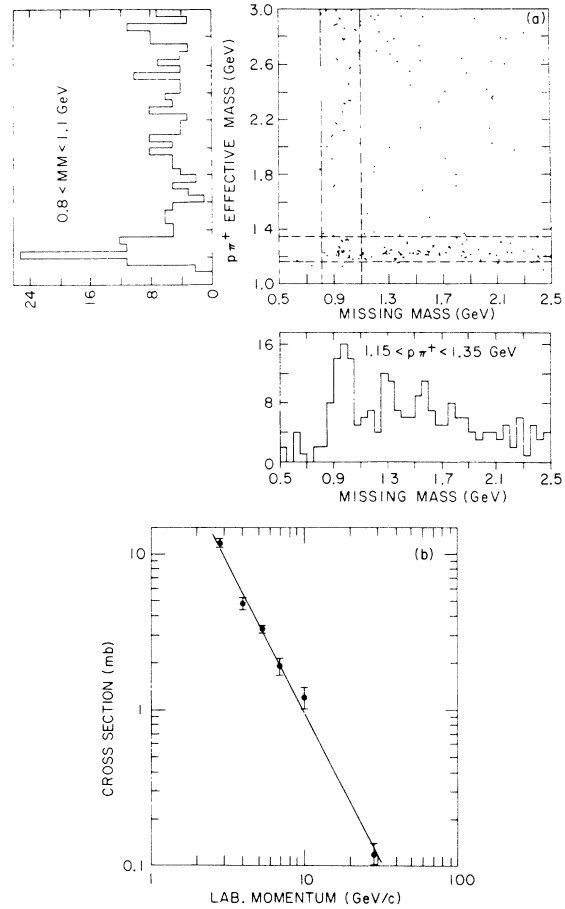


FIG. 3. (a) Missing mass  $MMn$  versus effective mass of  $p\pi^+$  in the reaction  $p + p \rightarrow p + \pi^+ + MMn$ . Also shown are projections of distributions within the bands indicated by dashed lines. (b) Energy dependence of the cross section for the reaction  $p + p \rightarrow \Delta^{++}(1238) + n$ .

isospin  $\frac{1}{2}$ , the ratio  $(n\pi^+)/(\rho\pi^0) = 2$  is required, which implies that the sum of  $n\pi^+$  and  $p\pi^0$  events is  $213 \pm 18$ . The remaining 22 events are presumably  $n\pi^+\pi^0$  and  $p\pi^0\pi^0$ , so that  $(n\pi^+\pi^0 + p\pi^0\pi^0)/(n\pi^+ + p\pi^0) \sim 0.1$ .

We conclude that our data show that the 1400 enhancement of the counter experiments is made up almost entirely of  $(n\pi^+ + p\pi^0)$  and that the isospin for the system is  $\frac{1}{2}$ .

(c) The effective mass of  $p\pi^+\pi^-$  of Reaction (6) is plotted in Figs. 2(d) and 2(e) for the regions  $t < 0.12$   $(\text{GeV}/c)^2$  and  $t > 0.12$   $(\text{GeV}/c)^2$ . In the low- $t$  region the  $p\pi^+\pi^-$  effective mass peaks in the low-mass end of the spectrum at  $\sim 1450$  MeV. Comparing this with  $n\pi^+$  at low  $t$  we see that the  $n\pi^+$  spectrum is centered at 1400, is much broader, and has a greater cross section in spite of the loss of events with very low  $t$  [see item (2)

above]. At large  $t$ , the  $p\pi^+\pi^-$  spectrum shows no peak at around 1450, but structure at higher masses including the 1600- to 1700-MeV region becomes more prominent. The  $p\pi^+\pi^-$  peak near 1450 MeV contains a large fraction of  $p\pi^+$  combinations constrained to be within the  $\Delta^{++}(1238)$  region by the small effective mass of the entire  $p\pi^+\pi^-$  system. Nevertheless, assuming that a large fraction of the low-mass events in  $p\pi^+\pi^-$  are  $\Delta^{++}(1238)\pi^-$ , the 1450 peak at low  $t$  could be an alternative decay of a 1400 isobar, the shift in the position of the peak to higher mass being due to the higher threshold for production.<sup>7</sup> Likewise, the structure at large  $t$  around 1600-1700 MeV could be interpreted as an inelastic decay of one or more resonances in the ~1690-MeV region.

(d) The final state  $\Delta^{++}(1238)n$  is detected in this experiment by using the technique described in item (2) applied to Reaction (8). A plot of the effective mass of  $p\pi^+$  vs  $(MMn)$  is shown in Fig. 3(a). The  $p\pi^+$  effective mass within the neutron band ( $0.8 < MMn < 1.1$  GeV) and the missing mass  $MMn$  within the  $\Delta^{++}(1238)$  band ( $1.15 < p\pi^+ < 1.35$  GeV) are projected, respectively, along the vertical and horizontal axes of the same figure. Selecting events above background in the region where the two bands cross gives the contribution of the final state  $\Delta^{++}(1238)n$ ; the result is a cross section of  $115 \pm 15 \mu\text{b}$ . To investigate the momentum dependence of the cross section we combine our cross section with data from lower energy bubble-chamber experiments.<sup>8</sup> A fit to the expression  $\sigma \sim P_{\text{lab}}^{-n}$  gives  $n = 1.91 \pm 0.08$ , which is consistent with the value  $n = 2$  expected for one-pion exchange.<sup>9</sup> The plot of  $\log(\text{cross section})$  vs  $\log(P_{\text{lab}})$  in Fig. 3(b) shows that data extending over a factor of 10 in  $P_{\text{lab}}$  agree well with our fit.

We gratefully acknowledge the cooperation given us by Dr. F. Turkot in interpreting results and in providing unpublished data. Thanks are due also to Dr. E. Hart who contributed ideas and gave substantial assistance in the early stages of this experiment, to Dr. W. Kernan and Dr. R. Ehrlich for discussions of mutual experimental difficulties, and to Dr. E. L. Berger for theoretical interpretation of results.

\*Work performed under the auspices of the U. S. Atomic Energy Commission.

<sup>1</sup>E. W. Anderson *et al.*, Phys. Rev. Letters **16**, 855 (1966); G. Belletini *et al.*, Phys. Letters **18**, 167 (1965); J. M. Blair *et al.*, Phys. Rev. Letters **17**, 789 (1966).

<sup>2</sup>K. J. Foley *et al.*, Phys. Rev. Letters **19**, 397 (1967).

<sup>3</sup> $t$  is defined as the smaller of the two possible values of the square of the four-momentum transfer in quasi-two-body  $pp$  interactions.

<sup>4</sup>For a calculation of this type for 6.0-GeV/c  $pp$  data see E. L. Berger *et al.*, Phys. Rev. Letters **20**, 964 (1968). Questions regarding resonance versus kinematic effect are discussed by G. F. Chew and A. Pignotti, Phys. Rev. Letters **20**, 1078 (1968).

<sup>5</sup>D. R. O. Morrison, Phys. Rev. **165**, 1699 (1968).

<sup>6</sup>For a discussion of some of these points see P. L. Connolly *et al.*, in Proceedings of the Third Topical Conference on Resonant Particles, Athens, Ohio, November, 1967 (to be published).

<sup>7</sup>Results from a 22-GeV/c  $pp$  experiment indicate strong evidence for a  $\Delta^{++}(1238)\pi^-$  structure at 1450; R. A. Jespersen *et al.*, "Observation of the  $p\pi\pi$  Decay Mode of the  $N_{1/2}^*(1400)$  Resonance in  $pp$  Interactions at 22 GeV/c" (to be published).

<sup>8</sup>G. Alexander *et al.*, "Elastic Scattering and Single Pion Production in  $pp$  Interactions at 6.92 BeV/c," Phys. Rev. (to be published). This article contains complete references to the lower energy data.

<sup>9</sup>See, e.g., E. Leader, Rev. Mod. Phys. **38**, 476 (1966), Eq. (2.13). Note for  $t \approx 0$ ,  $a_\pi \approx 0$  so Reggeization has little effect.